

Ernest L. Maynard · Xiangshi Tan · Paul A. Lindahl

## Autocatalytic activation of acetyl-CoA synthase

Received: 30 September 2003 / Accepted: 2 February 2004 / Published online: 11 March 2004  
© SBIC 2004

**Abstract** Acetyl-CoA synthase (ACS  $\equiv$  ACS/CODH  $\equiv$  CODH/ACS) from *Moorella thermoacetica* catalyzes the synthesis of acetyl-CoA from CO, CoA, and a methyl group of a corrinoid-iron-sulfur protein (CoFeSP). A time lag prior to the onset of acetyl-CoA production, varying from 4 to 20 min, was observed in assay solutions lacking the low-potential electron-transfer agent methyl viologen (MV). No lag was observed when MV was included in the assay. The length of the lag depended on the concentrations of CO and ACS, with shorter lags found for higher [ACS] and sub-saturating [CO]. Lag length also depended on CoFeSP. Rate profiles of acetyl-CoA synthesis, including the lag phase, were numerically simulated assuming an autocatalytic mechanism. A similar reaction profile was monitored by UV-vis spectrophotometry, allowing the redox status of the CoFeSP to be evaluated during this process. At early stages in the lag phase,  $\text{Co}^{2+}$  FeSP reduced to  $\text{Co}^+$  FeSP, and this was rapidly methylated to afford  $\text{CH}_3\text{-Co}^{3+}$  FeSP. During steady-state synthesis of acetyl-CoA, CoFeSP was predominately in the  $\text{CH}_3\text{-Co}^{3+}$  FeSP state. As the synthesis rate declined and eventually ceased, the  $\text{Co}^+$  FeSP state predominated. Three activation reductive reactions may be involved, including reduction of the A- and C-clusters within ACS and the reduction of the cobamide of CoFeSP. The B-, C-, and D-clusters in the  $\beta$  subunit appear to be electronically isolated from

the A-cluster in the connected  $\alpha$  subunit, consistent with the  $\sim 70$  Å distance separating these clusters, suggesting the need for an in vivo reductant that activates ACS and/or CoFeSP.

**Keywords** Acetyl-CoA synthesis · Carbon monoxide dehydrogenase · Corrinoid-iron-sulfur protein · Electron transfer · *Moorella thermoacetica*

**Abbreviations** ACS acetyl-CoA synthase, also known as CODH (carbon monoxide dehydrogenase) or CODH/ACS or ACS/CODH ·  $\text{CH}_3\text{-Co}^{3+}$  FeSP,  $\text{Co}^{2+}$  FeSP, and  $\text{Co}^+$  FeSP corrinoid-iron-sulfur protein with the cobalamin in the methylated 3+, unmethylated 2+, and unmethylated 1+ states · CoA coenzyme A · DTT dithiothreitol · H-THF or THF tetrahydrofolic acid or tetrahydrofolate · MT methyl transferase · MV methyl viologen

### Introduction

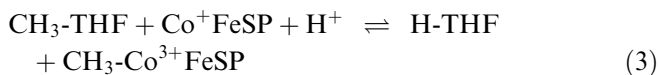
Acetyl-coenzyme A synthase/carbon monoxide dehydrogenase from the acetogenic bacteria *Moorella thermoacetica* (ACS  $\equiv$  ACS/CODH  $\equiv$  CODH/ACS) [1] is among the more exotic metalloenzymes, with two types of novel Ni-Fe-S active site clusters, an extensive tunneling network, and an organometallic catalytic mechanism [1]. ACS is an  $\alpha_2\beta_2$  tetramer that catalyzes two reactions, including the reversible reduction of  $\text{CO}_2$  to CO, reaction (1), and the synthesis of acetyl-CoA from CO, CoA, and the methyl group of a corrinoid-iron-sulfur protein (CoFeSP), reaction (2). CoFeSP is methylated by  $\text{CH}_3$ -tetrahydrofolate ( $\text{CH}_3$ -THF) in accordance with reaction (3), catalyzed by a methyltransferase (MT):



X. Tan · P. A. Lindahl (✉)  
Department of Chemistry, Texas A&M University,  
College Station, TX 77843-3255, USA  
E-mail: lindahl@mail.chem.tamu.edu  
Tel.: +1-979-8450956  
Fax: +1-979-8454719

E. L. Maynard  
Department of Biophysics and Biophysical Chemistry,  
The Johns Hopkins University School of Medicine, Baltimore,  
MD 21205, USA

P. A. Lindahl  
Department of Biochemistry and Biophysics,  
Texas A&M University, College Station, TX 77843, USA



The active site for CO<sub>2</sub> reduction, the [Ni Fe]:[Fe<sub>3</sub>S<sub>4</sub>] C-cluster, is located in the β subunit, while that for acetyl-CoA synthesis, the Ni<sub>d</sub>-Ni<sub>p</sub>-Fe<sub>4</sub>S<sub>4</sub> A-cluster, is located in the α subunit [2, 3]. Two Fe<sub>4</sub>S<sub>4</sub> clusters (B and D) are also located in the β subunit and serve to transfer electrons into or out of the C-cluster. A-clusters are ca. 70 Å from the B-, C-, and D-clusters. An extensive hydrophobic tunnel connects the A- and C-clusters, allowing CO generated at the C-cluster to migrate to the A-cluster without solvent exposure [2, 3, 4]. There is also evidence for the catalytic coupling of C- and A-clusters, affording an ordered sequential mechanism [5].

*Rhodospirillum rubrum* contains a carbon monoxide dehydrogenase (CODH<sub>Rr</sub>) homologous to the β subunit of ACS, including the same arrangement of B-, C-, and D-clusters. CODH<sub>Rr</sub> catalyzes reaction (1) but not (2). A lag phase in the onset of in vitro CO oxidation catalysis has been reported for CODH<sub>Rr</sub> [6]. This lag reflects an autocatalytic reduction of the enzyme, in which an active CODH<sub>Rr</sub> molecule activates an inactive CODH<sub>Rr</sub> molecule by reducing its C-cluster to a state that can bind and oxidize CO. Consistent with this, the length of the lag (ca. 0–100 s) depends on [CO], with lower concentrations affording longer lags. At [CODH] > 10 μM, the lag was independent of redox mediators such as methyl viologen (MV).

For acetyl-CoA synthesis, Co<sup>2+</sup>FeSP must also be reductively activated to the Co<sup>+</sup>FeSP state so that the cobalt achieves sufficient nucleophilicity to attack the methyl group of CH<sub>3</sub>-THF [7]. CoFeSP is a heterodimeric protein that contains a [Fe<sub>4</sub>S<sub>4</sub>]<sup>2+/+</sup> cluster in one subunit and a cobamide cofactor in the other [8, 9]. These cofactors each have midpoint potentials of ~ -500 mV vs. NHE. CoFeSP is reduced by ACS in the presence of CO in accordance with an apparent first-order rate constant of 0.88 min<sup>-1</sup> [10]. Electrons generated at the C-cluster of ACS are transferred to the Co of CoFeSP via its Fe<sub>4</sub>S<sub>4</sub> cluster [11].

ACS must also be reductively activated for acetyl-CoA synthesis [12, 13, 14]. This reduction is required for the proximal Ni (Ni<sub>p</sub>) to attain sufficient nucleophilicity to attack the methyl group of CH<sub>3</sub>-Co<sup>3+</sup>FeSP. Darnault et al. [2] proposed that reductive activation of ACS occurs when the proximal Ni of the A-cluster (Ni<sub>p</sub><sup>2+</sup>) is reduced to the zero-valent state, but there is no consensus that this state is achieved. For this paper, the site of reduction within the A-cluster is irrelevant. Both reductive activation of the A-cluster and of CoFeSP occur with E<sup>0</sup> ≈ -530 mV [11, 13, 14]. The C-cluster of ACS must also be reductively activated prior to binding and oxidizing CO [15], requiring potentials between -220 and -320 mV [6, 15].

When ACS catalyzes the synthesis of acetyl-CoA in vitro, either CO or CO<sub>2</sub> may be used as a substrate [4, 16]. When CO<sub>2</sub> is used, a low-potential redox mediator

such as MV must be added to activate ACS for catalysis and provide electrons for the catalytic reduction of CO<sub>2</sub>. However, when CO is used, such a reductant seems unnecessary, since CO also serves this function. In this paper, we report that, when CO is used as a substrate/reductant and MV is excluded, ACS exhibits a substantial lag period prior to the onset of acetyl-CoA synthesis. The effect of [CO] and [ACS] on lag times are investigated and modeled kinetically. Efforts are made to identify the event responsible for the lag.

## Materials and methods

ACS, CoFeSP, and MT, with molecular weights of 154,700 Da [17], 89,000 Da [18], and 57,280 Da [9], respectively, were purified from *M. thermoacetica* (ATCC 39073) cell paste [5, 16]. Protein purity was assessed by densitometric analysis of Coomassie Blue (Bio-Rad) stained SDS-PAGE gels. Specific activities for ACS-catalyzed CO oxidation [19] and acetyl-CoA synthesis [16] were 350 μmol min<sup>-1</sup> mg<sup>-1</sup> and 1.3 μmol min<sup>-1</sup> mg<sup>-1</sup>, respectively. CoFeSP and MT catalyzed the synthesis of acetyl-CoA with specific activities of 0.10 μmol min<sup>-1</sup> mg<sup>-1</sup> and 5.0 μmol min<sup>-1</sup> mg<sup>-1</sup>, respectively. The Biuret method [20] was used to determine protein concentrations. All experiments involving ACS and/or CoFeSP were performed under anaerobic conditions, as described previously [16].

### Lag experiments

ACS was rendered free of dithionite using a Sephadex G-25 column (1 cm×20 cm) equilibrated with buffer A (CO<sub>2</sub>-free [16] 50 mM MES, pH 6.3) supplemented with 1.0 mM dithiothreitol (DTT). CoFeSP was subjected to a similar chromatographic treatment, then titrated with thionin, and chromatographed again to remove excess thionin. MT was concentrated using a Centricon-10 (Amicon), diluted with 125 volumes of buffer A containing 1.0 mM DTT, and then reconcentrated. MV<sup>+</sup> was prepared enzymatically [16]. Concentrations of stock CH<sub>3</sub>-THF [21, 22] and CoA [23] solutions were calculated using their extinction coefficients. DTT was added (1.0 mM final) to the CoA solution to prevent oxidation.

### UV-vis monitoring of CoFeSP during catalysis

To a sealed Ar-filled quartz cuvette equipped with a magnetic “flea” stir bar was added CH<sub>3</sub>-THF (1.0 mM), CoFeSP (30 μM), and MT (10 μM) (all final concentrations). The Ar head-space of the cuvette was replaced with CO. After stirring the resulting solution for 20 min at 25 °C, acetyl-CoA synthesis was initiated by adding a CoA/ACS stock solution (in same buffer) to final concentrations of 1.0 mM and 0.27 μM, respectively. The cuvette was placed inside a UV/vis spectrophotometer (Spectral Instruments) and spectra (380–600 nm) were acquired every 10 s for 60 min. During the assay, the solution was continually stirred. Aliquots were removed periodically by syringe and assayed for acetyl-CoA by HPLC, as described [4]. Stopped-flow was performed essentially as described [5].

CO (MG Industries, research grade), CO<sub>2</sub> (MG Industries, anaerobic grade), and Ar were mixed with a flowmeter (MG Industries, series 7941-AS2 4-tube) and passed into a reaction vessel [16]. Henry's law constants for CO and CO<sub>2</sub> at 30 °C are 0.98 mM atm<sup>-1</sup> [23] and 31 mM atm<sup>-1</sup> [24], respectively. Acetyl-CoA synthase assays were performed as described [16].

## Kinetic simulations

A computer program was used to simulate acetyl-CoA versus time progress curves according to the mechanism depicted in the text. Ordinary differential equations (ODEs) describing the time-dependent concentration change of each component were numerically solved using a fifth-order Runge–Kutta method with adaptive step size control [25]. The sum of the squares of the residuals was iteratively minimized using an adaptive simulated annealing (ASA) algorithm [26].

## Results

CO-dependent acetyl-CoA synthase assays were performed in the presence and absence of MV. With 1 mM  $MV^+$  and 200  $\mu M$  CO (Fig. 1A, squares), acetyl-CoA was synthesized linearly with a specific activity of 0.24 units  $mg^{-1}$  (1 unit = 1  $\mu mol$  acetyl-CoA  $min^{-1}$ ). In the absence of MV, no acetyl-CoA was detected for the first 4.5 min after the reaction was initiated (Fig. 1A, circles). Subsequently, the rate of acetyl-CoA production increased until it approached that measured in the presence of MV.

The effect of [CO] on the lag was examined by performing a similar experiment under saturating CO conditions. In the presence of 1 mM  $MV^+$  and 1 atm (980  $\mu M$ ) CO, acetyl-CoA was linearly produced with a specific activity of 0.044 units  $mg^{-1}$  (Fig. 1B, squares), consistent with the inhibitory effects of CO [16]. In the absence of MV, a lag of  $\sim 20$  min was observed (Fig. 1B, circles), substantially longer than with lower CO

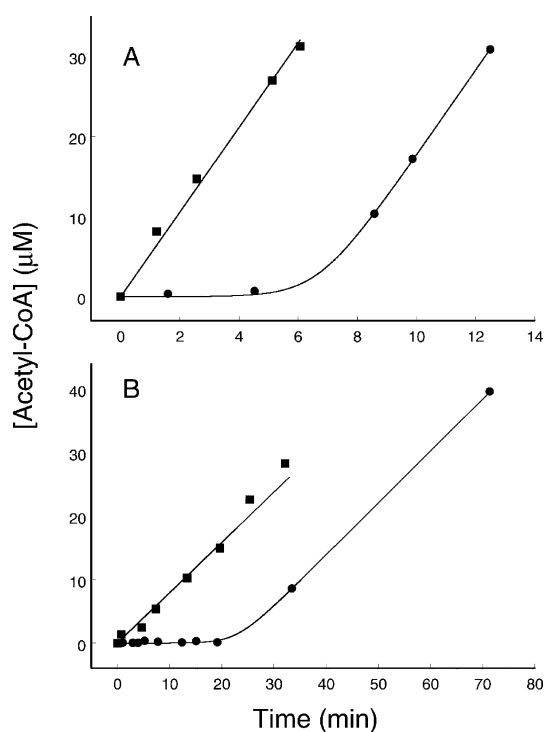


**Fig. 1** ACS-catalyzed synthesis of Acetyl-CoA with (squares) and without (circles) MV: **A** 200  $\mu M$  CO; **B** 980  $\mu M$  CO

concentrations. As in the previous experiment, the rate of acetyl-CoA synthesis eventually matched that obtained in the presence of MV.

The effect of [ACS] on lag time was investigated by a series of assays in the absence of MV and at 980  $\mu M$  [CO]. Doubling [ACS] from 0.13  $\mu M$  to 0.26  $\mu M$  shortened the lag from  $\sim 20$  min to  $\sim 15$  min (Fig. 2, circles vs. squares). Increasing [ACS] further caused lag times to drop. At the highest ACS concentration tested (1.46  $\mu M$ ), the lag time was  $\sim 2.5$  min (Fig. 2, inverted triangles). Using another batch of ACS, lags of  $\sim 15$  min were observed using [ACS] = 0.13  $\mu M$ , while no lag was noticeable using [ACS] = 0.3  $\mu M$ . Under the same conditions as the first batch, the steady-state activity of this batch was ca. four times higher, suggesting that observed lag times are sensitive to the activity of the enzyme as well as to protein concentration.

We wanted to determine whether the CoFeSP was involved in the lag phenomenon. CoFeSP exists in three spectrally distinct states, including as-isolated  $Co^{2+}$ -FeSP (470 nm shoulder), reduced  $Co^+$ -FeSP (sharp 390 nm feature), and methylated  $CH_3-Co^{3+}$ -FeSP (broad 450 nm feature). The  $Fe_4S_4$  cluster is oxidized (2+ core state) in the  $Co^{2+}$ -FeSP state and reduced (1+ core state) in the  $Co^+$ -FeSP state. Only  $Co^+$  can accept a methyl group from  $CH_3$ -THF to form  $CH_3-Co^{3+}$ -FeSP, which then donates its methyl group to ACS for the synthesis of acetyl-CoA. The spectral properties of CoFeSP as well as the concentration of acetyl-CoA were simultaneously measured (see Materials and methods) during and after the lag phase (Fig. 3). The spectrum obtained prior to initiating the reaction by adding ACS and CoA to the CO-saturated assay solution was similar to that of unactivated  $Co^{2+}$ -FeSP [8]. A similar comparison to known spectral states revealed that, during the lag phase,  $Co^{2+}$ -FeSP was converted into  $CH_3-Co^{3+}$ -FeSP without buildup of the  $Co^+$ -FeSP state. Since the intermediate  $Co^+$  form was not detected, it must have rapidly reacted with  $CH_3$ -THF to form

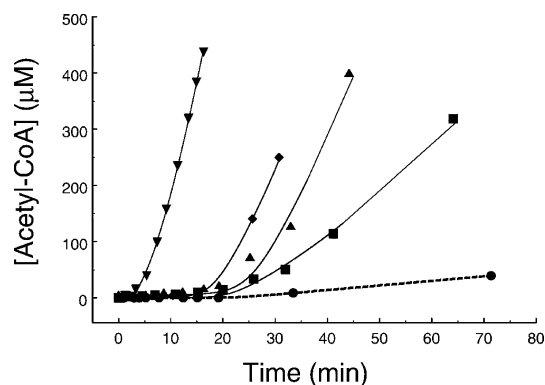


**Fig. 2** Effect of changing [ACS] on lag time in acetyl-CoA synthesis: [CO] = 980  $\mu M$  and [ACS] = 1.46  $\mu M$  (inverted triangles), 0.53  $\mu M$  (diamonds), 0.37  $\mu M$  (triangles), 0.26  $\mu M$  (squares), and 0.13  $\mu M$  (circles). Circles and the dashed line are replots of the data and line in Fig. 1B

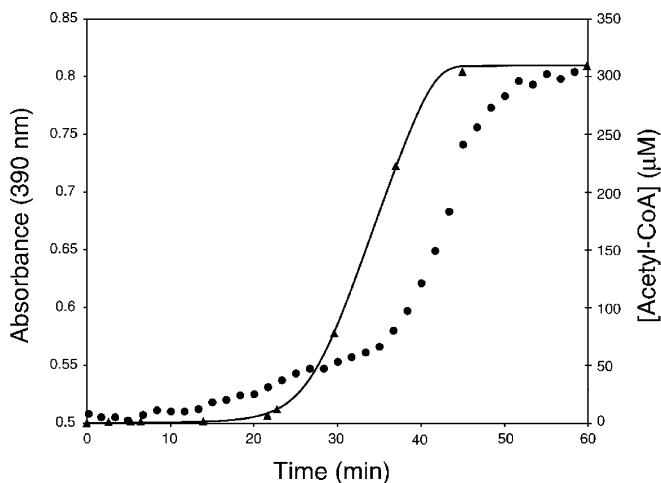


**Fig. 3** Redox status of the CoFeSP during and after the lag phase. The 390 nm (*circles*) spectral features of CoFeSP are plotted along with the concentration of acetyl-CoA (*triangles*) as a function of time. The *solid line* is a best-fit to the acetyl-CoA data

$\text{CH}_3\text{-Co}^{3+}\text{FeSP}$ . The  $\text{CH}_3\text{-Co}^{3+}\text{FeSP}$  form dominated during the steady-state catalytic region, where acetyl-CoA was synthesized at a constant rate. This indicates that the transfer of methyl from  $\text{CH}_3\text{-THF}$  to  $\text{Co}^+\text{FeSP}$  is fast relative to the transfer of methyl from  $\text{CH}_3\text{-Co}^{3+}\text{FeSP}$  to ACS and confirms the design of the assay: that the reaction should be limited by ACS and not by methyl transfer between  $\text{Co}^+\text{FeSP}$  and  $\text{CH}_3\text{-THF}$ . Acetyl-CoA synthesis halted once its concentration reached  $\sim 300\ \mu\text{M}$ ; at this point,  $\text{CH}_3\text{-Co}^{3+}\text{FeSP}$  converted back to  $\text{Co}^+\text{FeSP}$ .

An additional experiment was designed to address CoFeSP's role in the reaction(s) giving rise to the lag phenomenon. Using stopped-flow methods, CO-reduced ACS was reacted with  $\text{Co}^{2+}\text{FeSP}$  and the product  $\text{Co}^+\text{FeSP}$  was monitored by UV-vis spectroscopy. The kinetics of  $\text{Co}^{2+}\text{FeSP}$  reduction was slow, requiring over 30 min for completion (Fig. 4). A slight lag in the onset of  $\text{Co}^{2+}\text{FeSP}$  reduction, corresponding to  $\sim 30\ \text{s}$ , was observed. Under these conditions, a lag in acetyl-CoA synthesis of  $\sim 15\ \text{min}$  would be expected.

No lag was observed when as-isolated CoFeSP was pre-incubated in 1 atm CO,  $\text{CH}_3\text{-THF}$ , MT, and a small amount of ACS ( $0.1\ \mu\text{M}$  final concentration) for 5 h before initiating the reaction with CoA and a larger

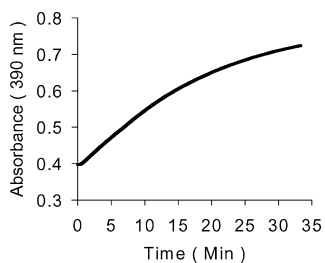


**Fig. 4** CoFeSP ( $60\ \mu\text{M}$ ) in CO-saturated buffer A was reacted with CO-saturated buffer A containing  $0.6\ \mu\text{M}$  ACS. The reaction was monitored at 390 nm

amount of ACS ( $0.38\ \mu\text{M}$ ) (Fig. 5). Nor was a substantial lag observed when the entire amount of ACS was pre-incubated with CoFeSP prior to initiating the reaction with CoA (Fig. 6, triangles). A lag time of  $\sim 10\ \text{min}$  (half of that observed in the control; Fig. 6, circles) was obtained when  $\text{CH}_3\text{-Co}^{3+}\text{FeSP}$  rather than CoFeSP was used in the standard assay (initiating the reaction with ACS and CoA) (Fig. 6, squares).

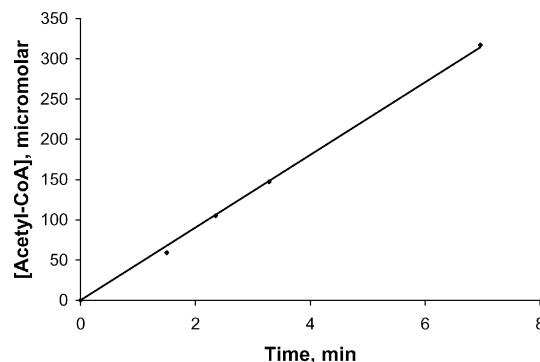


**Fig. 5** Pre-Incubation of CoFeSP prior to acetyl-CoA synthase activity assay: CoFeSP ( $30\ \mu\text{M}$ , all concentrations are final),  $\text{CH}_3\text{-THF}$  ( $2.0\ \text{mM}$ ), MT ( $10\ \mu\text{M}$ ), MES ( $50\ \text{mM}$ , pH 6.3), and ACS ( $0.1\ \mu\text{M}$ ) were added to a reaction vessel which was then flushed for 15 min with 1 atm CO. After 5 h incubation in the glove box, the catalytic synthesis of acetyl-CoA was initiated by addition of a solution of CoA and ACS ( $1.0\ \text{mM}$  and  $0.38\ \mu\text{M}$ , respectively, yielding a  $400\ \mu\text{L}$  reaction volume). Aliquots ( $50\ \mu\text{L}$ ) were removed by syringe at various times and analyzed for acetyl-CoA by reversed-phase HPLC

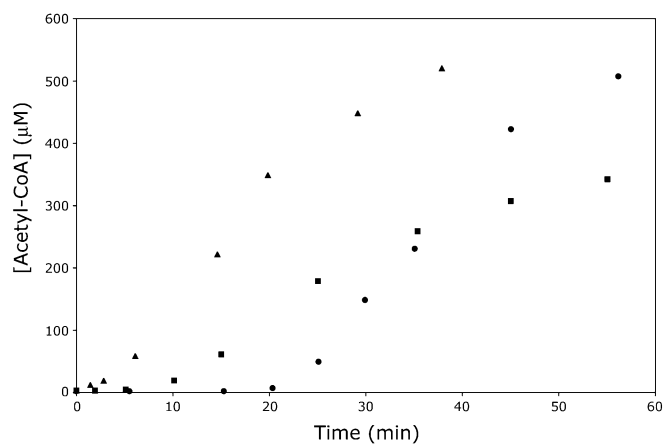


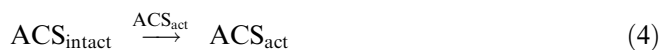
**Fig. 6** Acetyl-CoA synthesis initiated by adding CoA and ACS simultaneously (*circles*) or CoA alone (*triangles*). Other conditions were as described in Materials and methods. *Circles* represent the control, as ACS and CoA are typically added together to initiate reactions. In this experiment,  $0.272\ \mu\text{M}$  ACS, 1 atm CO, and no MV were used. *Squares* are the same as circles, except that  $\text{CH}_3\text{-CoFeSP}$  replaced CoFeSP. *Triangles* are the same as circles, except that ACS was pre-incubated in the assay solution for 40 min before CoA was added to initiate acetyl-CoA synthesis

## Discussion

In vitro acetyl-CoA synthesis involves a complicated interplay of three proteins, including ACS, CoFeSP, and MT (as well as substrates CoA, CH<sub>3</sub>-THF, CO or CO<sub>2</sub>). Three reductive activation reactions are required for this system to catalyze the synthesis of acetyl-CoA. First, the C-cluster of ACS must be reduced to a state capable of binding and oxidizing CO to CO<sub>2</sub> (we believe that this state corresponds to C<sub>red1</sub>). Co<sup>2+</sup>FeSP must also be reduced to the Co<sup>+</sup>FeSP state so that it can react with CH<sub>3</sub>-THF and form CH<sub>3</sub>-Co<sup>3+</sup>FeSP. Finally, the A-cluster of ACS must be reduced so that it can accept a methyl group from CH<sub>3</sub>-Co<sup>3+</sup>FeSP. When CO is the exclusive reductant, the C-cluster *must* be activated before CoFeSP and the A-cluster are activated, as these latter activations use electrons generated from the oxidation of CO.

The presence of a lag in the onset of acetyl-CoA synthesis in assays lacking MV indicates that ACS and/or CoFeSP are largely unactivated when injected into the assay solution. MV probably allows the rapid activation of these proteins (within the time of manual mixing) by mediating the CO-dependent reduction. In the absence of MV, the same reductive activation processes must occur, and our results indicate that they occur at a much slower rate.

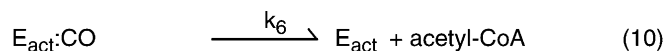
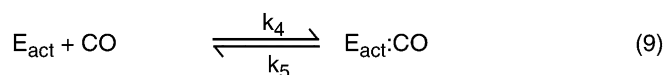
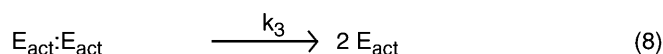
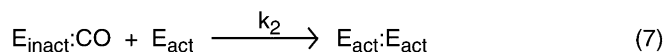
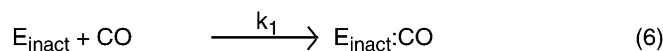
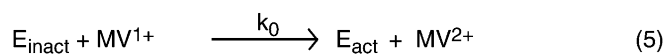
The dramatic increase in activity after a lengthy lag suggests that this process is autocatalytic with respect to ACS (or with CoFeSP or both). The effect of [ACS] on lag times is congruent with its role as an autocatalyst, with higher concentrations affording shorter lag times in a nonlinear fashion. This would require that a minute fraction of ACS (0.1% is assumed in our simulations described below) would be active initially, and that this portion would catalyze the activation of the remaining inactive ACS molecules, as in reaction (4):



Once this self-catalyzed activation reached completion, all ACS molecules would be active and the rate of acetyl-CoA synthesis would match that when MV<sup>+</sup> was included in the assay solution, as observed.

The effect of [CO] is also qualitatively comprehensible. The inverse relationship between the length of the lag and [CO] probably arises from the fact that CO is an uncompetitive substrate inhibitor at high concentrations (100–980 μM) [16]. CO at low concentrations shortens the lag because it acts primarily as a substrate at these concentrations, while CO at high concentrations lengthens the lag because it inhibits catalysis.

We modeled these processes using reactions (5)–(10):



This model is simplistic but provides some qualitative insight. “E” could be viewed alternatively as ACS or as an acetyl-CoA synthase *complex* composed of ACS and CoFeSP. Inhibitory effects of CO are not included, and substrates and products not pertinent to the model or varied in the experiments are excluded. Thus CO is oxidized to CO<sub>2</sub> in reaction (7) but CO<sub>2</sub> is not included as a product. E<sub>act</sub>:CO reacts with a methyl group and CoA, but these substrates are constant and are thus not included.

According to the model, either MV<sup>+</sup> or CO converts inactive E into its catalytically active form. The MV-dependent reaction (5) is written as a second-order process (involving one MV<sup>+</sup>), but this should not be misconstrued as implying that activation is actually a one-electron process. The CO-dependent reactions (6)–(8) together constitute an autocatalytic group. Autocatalytic activation of E<sub>inact</sub> occurs when it binds CO (reaction 6) and E<sub>act</sub> (reaction 7), promoting dissociation of two E<sub>act</sub> molecules (reaction 8). Formation of the E<sub>act</sub>:E<sub>act</sub> complex and subsequent redox chemistry are simplistically represented as a single step, reaction (7). The result of either pathway is the formation of E<sub>act</sub>, which catalytically binds substrate and forms product, reactions (9) and (10).

Linear acetyl-CoA versus time data from experiments where MV was present (Fig. 1A and B, squares) were simulated using a standard Michaelis–Menten model (i.e.  $k_1$ ,  $k_2$ , and  $k_3$  were set equal to zero). The model was optimized to the data sets, affording the solid lines in the figures. Best-fit rate constants are given in Table 1. The MV-mediated reductive activation rate was quite fast, as evidenced by the lack of a lag phase. Not surprisingly, the best-fit value for  $k_0$  was large, ranging from 13 μM<sup>-1</sup> min<sup>-1</sup> (200 μM CO) to 19 μM<sup>-1</sup> min<sup>-1</sup> (980 μM CO). This is in accordance with reductive activation rates measured previously with Ti<sup>3+</sup> citrate [27]. Some best-fit

**Table 1** Best-fit rate constants for the model represented in reactions (5)–(10)

[MV <sup>+</sup> ] (mM)	[ACS] ( $\mu\text{M}$ )	[CO] ( $\mu\text{M}$ )	$\text{E}_{\text{inact}} \xrightarrow{\text{MV}^+} \text{E}_{\text{det}}$		$\text{E}_{\text{inact}} : \text{CO} \xrightarrow{\text{CO}} \text{E}_{\text{inact}} : \text{CO}$	$\text{E}_{\text{inact}} : \text{CO} \xrightarrow{\text{CO}} \text{E}_{\text{det}} : \text{CO}$	$\text{E}_{\text{det}} \xrightarrow{\text{CO}} \text{E}_{\text{det}} : \text{CO}$	$\text{E}_{\text{det}} : \text{CO} \rightarrow \text{E}_{\text{det}}$	$\text{E}_{\text{det}} : \text{CO} \rightarrow \text{E}_{\text{det}}$	$\text{E}_{\text{det}} : \text{CO} \rightarrow \text{E}_{\text{det}} + \text{P}$
			$k_0$ ( $\mu\text{M}^{-1}\text{min}^{-1}$ )	$k_1 \times 10^{-5}$ ( $\mu\text{M}^{-1}\text{min}^{-1}$ )						
1.0	0.13	200	13	0 <sup>a</sup>	0	0	0	0	71	42
1.0	0.13	980	19	0	0	0	0	0	190	5.9
0	0.13	200	—	350	860	860	860	860	0.11	41
0	0.13	980	—	14	980	980	980	980	1.5	6.2
0	0.26	980	—	2.4	510	510	510	510	0.093	45
0	0.37	980	—	2.0	430	430	430	430	0.13	110
0	0.53	980	—	2.0	490	490	490	490	0.58	96
0	1.5	980	—	2.0	770	770	770	770	0.15	180
0	0.27	310 <sup>b</sup>	—	9.3	180	180	180	180	0.071	150

<sup>a</sup>A Michaelis–Menten kinetic model was fit to the data (see text for details)<sup>b</sup>Owing to a different experimental setup, [CO] was allowed to float (see text for details)

values varied from one fit to another, in some cases by two orders of magnitude (e.g.  $k_1$ , the second-order rate constant for CO binding to inactive enzyme). Clearly, a more sophisticated model is required for quantitative satisfaction, but our simple model provides support for a CO-dependent autocatalytic activation of ACS.

Rate constant  $k_1$  is about  $10^5$  times smaller than that for MV-mediated activation. This indicates that MV-mediated activation is much faster than that mediated by CO and implies that MV activates the ACS complex within milliseconds after mixing. The simulated lag phase is strongly dependent on the value of  $k_1$ , with larger values giving rise to shorter lag times. When [ACS] was fixed at  $0.13 \mu\text{M}$ , best-fit  $k_1$  decreased  $\sim 25\times$  when [CO] increased from  $200 \mu\text{M}$  to  $980 \mu\text{M}$ . In an earlier study, we found that CO is an uncompetitive inhibitor of the steady-state synthesis of acetyl-CoA [16]. Under higher CO concentrations, the fraction of ACS that is active (and thus able to activate other inactive molecules) is likely sequestered by CO to form an inhibited complex. When [CO] was fixed at  $980 \mu\text{M}$ , best-fit  $k_1$  decreased  $\sim 6\times$  when [ACS] increased from  $0.13 \mu\text{M}$  to  $0.26 \mu\text{M}$ .

Determining the detailed mechanism of reductive activation is beyond the scope of this study; specifically, we are unable to determine unequivocally which of the three activation steps required for acetyl-CoA synthesis is responsible for the lag. The fact that a CO-sensitive lag has also been observed in  $\text{CODH}_{\text{Rr}}$  suggests that the lag observed here might be dictated by the reduction of the C-cluster. However, the lengths of the lags are substantially longer (seconds for  $\text{CODH}_{\text{Rr}}$  versus minutes for ACS) and the effect of CO is different (higher CO concentrations shortened the  $\text{CODH}_{\text{Rr}}$  lag while they lengthen the ACS<sub>Mt</sub> lags) and congruent with the inhibitory effects of CO on acetyl-CoA synthesis. The large distance separating A- and C-clusters, the lack of an electron transfer pathway between these centers, and the ability of a small (i.e. rapidly migrating) redox mediator to abolish the lag suggest that the two centers are electronically isolated and that an autonomous reductant (e.g. MV or a separate ACS molecule in vitro or an unidentified oxidoreductase in vivo) might be required to activate ACS. This runs counter to our previous assumption (see fig. 12 of [15]) in which electrons were suggested to transfer *intramolecularly* from the C-cluster to the A-cluster of the same  $\alpha\beta$  unit. Rather, our results support the conclusion of Doukov et al. [3] that “direct electron transfer between these clusters is unlikely to occur at a rate sufficient to explain the reductive activation of the acetyl-CoA synthase complex (including CoFeSP) occurs *intermolecularly*. Finally, the lack of a lag phase in the experiment of Fig. 5 could suggest that reductive activation and methylation of  $\text{Co}^{2+}\text{FeSP}$  may be slow, analogous to that required for reductive activation of methionine synthase [28]. Further studies will be required to understand this intriguing phenomenon on the mechanistic level.

**Acknowledgements** The National Institutes of Health (GM46441 to P.A.L. and GM08523 to E.L.M.) sponsored this study.

---

## References

1. Lindahl PA (2002) *Biochemistry* 41:2097–2105
2. Darnault C, Volbeda A, Kim EJ, Legrand P, Vernede X, Lindahl PA, Fontecilla-Camps JC (2003) *Nat Struct Biol* 10:271–279
3. Doukov TI, Iverson TM, Seravalli J, Ragsdale SW, Drennan CL (2002) *Science* 298:567–572
4. Maynard EL, Lindahl PA (1999) *J Am Chem Soc* 121:9221–9222
5. Maynard EL, Lindahl PA (2001) *Biochemistry* 40:13262–13267
6. Heo J, Halbeib CM, and Ludden PW (2001) *Proc Natl Acad Sci USA* 98:7690–7693
7. Seravalli J, Zhao SY, Ragsdale SW (1999) *Biochemistry* 38:5728–5735
8. Ragsdale SW, Lindahl PA, Munck E (1987) *J Biol Chem* 262:14289–14297
9. Roberts DL, James-Hagstrom JE, Garvin DK, Gorst CM, Runquist JA, Baur JR, Haase FC, Ragsdale SW (1989) *Proc Natl Acad Sci USA* 86:32–36
10. Menon S, Ragsdale SW (1998) *Biochemistry* 37:5689–5698
11. Menon S, Ragsdale SW (1999) *J Biol Chem* 274:11513–11518
12. Pezacka E, Wood H (1988) *J Biol Chem* 263:16000–16006
13. Lu W, Harder SR, Ragsdale SW (1990) *J Biol Chem* 265:3124–3133
14. Barondeau DP, Lindahl PA (1997) *J Am Chem Soc* 119:3959–3970
15. Anderson ME, Lindahl PA (1994) *Biochemistry* 33:8702–8711
16. Maynard EL, Sewell C, Lindahl PA (2001) *J Am Chem Soc* 123:4697–4703
17. Morton TA, Rundquist AR, Ragsdale SW, Shanmugasundaram T, Wood HG, Ljundahl LG (1991) *J Biol Chem* 266:23824–23828
18. Lu WP, Schiau I, Cunningham JR, Ragsdale SW (1993) *J Biol Chem* 268:5605–5614
19. Shin W, Lindahl PA (1993) *Biochim Biophys Acta* 1161:317–322
20. Pelley JW, Garner CW, Little GH (1978) *Anal Biochem* 86:341–343
21. Gupta VS, Huennekens FM (1967) *Arch Biochem Biophys* 120:712–718
22. Blair JA, Saunders KJ (1970) *Anal Biochem* 34:376–381
23. Budavari S (1989) *The Merck index*, 11th edn. Merck, Rahway, NJ
24. Butler JN (1982) *Carbon dioxide equilibria and their applications*. Addison-Wesley, Reading, Mass
25. Shoup TE (1984) *Applied numerical methods for the microcomputer*. Prentice-Hall, Englewood Cliffs, NJ
26. Ingber L (1996) *Control Cybernet* 25:33–54
27. Tan X, Sewell C, Lindahl PA (2002) *J Am Chem Soc* 124:6277–6284
28. Jarrett, JT, Hoover, DM, Ludwig, ML, Matthews, RG (1998) *Biochemistry* 37:12649–12658